Nuclear Inst, and Methods in Physics Research B 416 (2018) 41–49

Contents lists available at ScienceDirect

Nuclear Inst. and Methods in Physics Research B

journal homepage: www.elsevier.com/locate/nimb

Evaluation of fusion-evaporation cross-section calculations

B. Blank[a,b,*], G. Canchel[a], F. Seis[a,1], P. Delahaye[c]

[a] Centre d'Etudes Nucléaires de Bordeaux Gradignan, 19 Chemin du Solarium, CS10120, F-33175 Gradignan Cedex, France
[b] ISOLDE/CERN, EP Department, CH-1211 Geneve 23, Switzerland
[c] Grand Accélérateur National d'Ions Lourds, Bd Henri Becquerel, BP 55027, 14076 CAEN Cedex 05, France

ARTICLE INFO

Keywords:
Fusion-evaporation reactions
Comparison experiment – calculations

ABSTRACT

Calculated fusion-evaporation cross sections from five different codes are compared to experimental data. The present comparison extents over a large range of nuclei and isotopic chains to investigate the evolution of experimental and calculated cross sections. All models more or less overestimate the experimental cross sections. We found reasonable agreement by using the geometrical average of the five model calculations and dividing the average by a factor of 11.2. More refined analyses are made for example for the ^{100}Sn region.

1. Introduction

On Earth, 255 stable nuclides are available for nuclear physics studies. In addition, 31 quasi stable nuclides having a half-life comparable to or longer than the age of the Earth exist. All other nuclei must be created in order to be usable for experimental studies. Different types of nuclear reactions exist to produce these unstable and radioactive nuclei.

Two methods can be used to create basically all bound or quasi bound (i.e. bound for a short laps of time) nuclei lighter than the projectile or target nuclei: spallation or fragmentation. Spallation reactions are usually induced by light particles (protons or neutrons) on heavier stable target nuclei. In these spallation reactions, the incident light projectile ejects nucleons from the target nucleus by nucleon-nucleon collisions and the excited fragment (often called pre-fragment) evaporates light particles (protons, neutrons, α particles) to get rid of excitation energy. With e.g. incident proton energies of a few hundred MeV up to 1 or 2 GeV, basically all nuclei, bound or quasi bound, but lighter than the target nucleus itself, can be produced. However, as these spallation reactions are basically always "thick-target" reactions, the reaction products have to diffuse out of the target to become useful. As this takes some time and depends very sensitively on the chemistry of the element of interest, short-lived nuclides of condensable elements are very difficult to produce by this means.

Fragmentation reactions employ heavy-ion induced reactions on different heavy-ion targets. Therefore, target as well as projectile fragmentation can be used. Target fragmentation suffers from the same problem as spallation reactions: the products have to diffuse from the target itself. Therefore, this process is again limited to relatively volatile isotopes with sufficiently long half-lives. In projectile fragmentation reactions, one can use "thin targets" which allows the products to recoil out of the target due to the incident projectile energy. This approach is basically universal and allows all nuclides lighter than the projectile to be produced. However, there are at least two drawbacks of projectile fragmentation: i) it needs high-energy heavy-ion accelerators and ii) the beam quality of these fragment beams is rather bad.

In deep-inelastic or transfer reactions, two heavy nuclei interact with each other at energies around the Fermi energy (typically 20–60 MeV/A) and nucleons are transferred from one nucleus to the other producing thus more or less neutron-rich or neutron-deficient isotopes. However, as the number of nucleons transferred is limited, mainly nuclei relatively close to stability in the vicinity of the projectile and the target nuclei are produced.

In nuclear fission, a very heavy nucleus, e.g. ^{238}U or ^{252}Cf, fissions by creating two medium-mass nuclides. This fission process can be induced (e.g. by proton, neutron or γ-ray impact) or spontaneous. Due to the curvature of the nuclear valley of stability, the heavy fissioning nuclei have always an excess of neutrons compared to lighter nuclei. Therefore, nuclear fission always produces neutron-rich isotopes in the mass range of A ≈ 50–170.

Finally, neutron-deficient nuclides can be produced by fusing two lighter nuclei. In this case, the situation is reversed compared to fission. The light stable nuclei that interact are proton-rich compared to the heavier nuclei in the valley of stability. For example, the reaction of a stable ^{40}Ca nucleus with a stable ^{58}Ni nucleus produces as the compound nucleus, i.e. the sum of all nucleons, ^{98}Cd, a nucleus which is 8 neutrons more neutron-deficient than the most neutron-deficient stable isotope of the element cadmium.

* Corresponding author at: Centre d'Etudes Nucléaires de Bordeaux Gradignan, 19 Chemin du Solarium, CS10120, F-33175 Gradignan Cedex, France.
E-mail address: blank@cenbg.in2p3.fr (B. Blank).
[1] Summer student at CENBG.

https://doi.org/10.1016/j.nimb.2017.12.003
Received 18 September 2017; Received in revised form 4 December 2017; Accepted 4 December 2017
Available online 10 December 2017
0168-583X/ © 2018 The Authors. Published by Elsevier B.V. This is an open access article under the CC BY license (http://creativecommons.org/licenses/BY/4.0/).

Table 1
Experimental cross sections from literature. Given are the mass and charge number of the nuclei of interest, the mass and charge number of the projectile and target nuclei, respectively, the incident beam energy, the experimental cross section and its error if available, and the reference.

A	Z	A_p	Z_p	A_t	Z_t	E (MeV)	Cross section (mb)	Error (mb)	Ref.
Light N ≈ Z nuclei									
64	30	12	6	54	26	37	1.60E+02	7.00E+00	[21]
64	31	54	26	12	6	150	7.90E+01		[22]
64	32	40	20	27	13	102	4.00E−01	6.00E−02	[23]
64	32	54	26	12	6	165	6.40E−01	7.00E−02	[21]
64	32	54	26	12	6	150	3.40E−01	9.00E−02	[22]
64	32	54	26	12	6	165	5.00E−01	3.00E−01	[24]
64	32	12	6	58	28	40	2.00E−01	5.00E−02	[25]
68	34	58	28	12	6	175	3.80E−02	1.60E−02	[24]
68	34	58	28	12	6	220	2.00E−01	5.00E−02	[26]
72	36	16	8	58	28	55	1.00E−01	3.00E−02	[25]
72	36	58	28	16	8	170	6.00E−02	2.50E−02	[27]
76	38	54	26	24	12	175	1.00E−02	5.00E−03	[24]
80	40	58	28	24	12	190	1.00E−02	5.00E−03	[28]
80	39	58	28	24	12	190	2.00E+00	1.00E+00	[28]
80	38	58	28	24	12	190	4.40E+01	4.00E+00	[28]
^{100}Sn region									
95	45	58	28	50	24	250	1.10E+00	4.00E−01	[29]
97	45	58	28	50	24	250	3.40E+00	2.00E−01	[29]
98	46	58	28	50	24	250	2.20E+01	2.00E+00	[29]
98	47	58	28	50	24	250	3.00E−01	6.00E−02	[29]
99	47	58	28	50	24	250	3.60E+00	4.00E−01	[29]
99	48	58	28	50	24	249	3.20E−02	2.00E−02	[30]
99	48	58	28	50	24	249	3.20E−02	2.00E−02	[30]
99	48	50	24	58	28	225	2.50E−02	8.00E−03	[30]
99	48	58	28	58	28	348	1.10E−02	8.00E−03	[30]
99	48	58	28	58	28	371	2.80E−02	2.10E−02	[30]
99	48	58	28	58	28	394	3.10E−02	2.00E−02	[30]
100	47	58	28	50	24	250	3.90E+00	2.00E−01	[29]
100	47	50	24	58	28	225	3.90E+00		[29]
100	48	50	24	58	28	225	1.00E+00		[31]
100	49	50	24	58	28	225	1.00E−03		[31]
100	49	58	28	50	24	319	2.60E−03		[30]
100	49	58	28	58	28	325	8.00E−04		[30]
100	49	58	28	58	28	348	1.70E−03		[30]
100	49	58	28	58	28	371	1.70E−03		[30]
100	49	58	28	58	28	394	1.60E−03		[30]
100	50	50	24	58	28	225	4.00E−05		[31]
101	47	58	28	50	24	250	4.70E+01	3.00E+00	[29]
101	48	58	28	50	24	250	1.80E+01	2.00E+00	[29]
101	50	58	28	50	24	249	1.60E−05	4.00E−06	[30]
101	50	58	28	50	24	250	1.00E−05		[30]
101	50	58	28	58	28	325	9.00E−06	4.00E−06	[30]
101	50	58	28	58	28	348	1.30E−05	3.00E−06	[30]
101	50	58	28	58	28	371	2.80E−05	1.00E−05	[30]
101	50	58	28	58	28	394	7.00E−06	4.00E−06	[30]
102	48	58	28	50	24	250	6.30E+01	1.90E+01	[29]
102	49	58	28	50	24	249	9.00E−01	5.00E−01	[30]
102	49	58	28	50	24	249	1.30E+00	7.00E−01	[30]
102	49	58	28	50	24	348	1.10E+00	6.00E−01	[30]
102	49	58	28	58	28	325	1.20E+00	6.00E−01	[30]
102	49	58	28	58	28	348	1.20E+00	6.00E−01	[30]
102	49	58	28	58	28	348	7.00E−01	3.00E−01	[30]
102	49	58	28	58	28	371	1.00E+00	5.00E−01	[30]
102	49	58	28	58	28	394	9.00E−01	4.00E−01	[30]
102	50	58	28	52	24	225	2.00E−03		[32]
103	47	58	28	50	24	250	3.60E+00	4.00E−01	[29]
103	48	58	28	50	24	250	2.70E+01	2.00E+00	[29]
103	49	58	28	50	24	250	6.40E+00	8.00E−01	[29]
104	48	58	28	50	24	250	1.79E+02	7.00E+00	[29]
104	49	58	28	50	24	250	5.80E+01	1.60E+01	[29]
104	50	58	28	50	24	250	1.80E+00	2.00E−01	[29]
105	49	58	28	50	24	250	1.16E+02	6.00E+00	[29]
105	50	58	28	50	24	250	1.00E+01	2.00E+00	[29]
Ba nuclei									
114	56	58	28	58	28	222−−248	2.00E−04	1.00E−04	[33]
114	56	58	28	58	28	203−−244	2.00E−04	1.00E−04	[34]
116	56	58	28	60	28	209−−249	3.00E−03	1.00E−03	[34]
116	56	58	28	63	29	249−−284	8.00E−04	4.00E−04	[34]
117	56	58	28	63	29	249−−284	5.50E−02	2.00E−02	[34]
118	56	58	28	63	29	249−−284	1.90E−02	6.00E−03	[34]
Heavier nuclei									
171	79	78	36	96	44	361	1.10E−03		[35]
171	79	78	36	96	44	359	2.00E−03		[35]
171	79	78	36	96	44	363	6.00E−04		[35]
170	79	78	36	96	44	386	9.00E−05		[35]
173	80	78	36	102	46	384	4.00E−06		[35]
172	80	78	36	96	44	361	4.00E−06		[35]
171	80	78	36	96	44	361	2.00E−06		[35]
176	81	78	36	102	46	384	3.00E−06		[35]
172	80	78	36	96	44	375	9.00E−06		[36]
173	80	80	36	96	44	400	1.50E−05		[36]
174	80	80	36	96	44	375	3.30E−04		[36]
Proton emitter: pn channel									
185	83	92	42	95	42	410	1.00E−04		[37]
185	83	92	42	95	42	420	6.00E−05		[38]
Proton emitter: p2n channel									
109	53	58	28	54	26	195	1.00E−02		[39]
109	53	58	28	54	26	220	1.60E−02	4.00E−03	[40]
109	53	58	28	54	26	240	3.00E−03		[41]
109	53	58	28	54	26	229	5.00E−02		[42]
109	53	58	28	54	26	250	4.00E+01	$+4.00E+01$ $-2.00E+01$	[43]
109	53	58	28	58	28	250	3.00E+01	$+3.00E+01$ $-1.50E+01$	[43]
113	55	58	28	58	28	250	3.00E+01		[43]
147	69	58	28	92	42	260	1.80E−02		[44]
151	71	58	28	96	44	266	7.00E−02	1.00E−02	[45]
161	75	58	28	106	48	270	6.30E−03	1.80E−03	[46]
167	77	78	36	92	42	357	1.10E−01		[47]
171	79	78	36	96	44	389	2.00E−03		[47]
171	79	78	36	96	44	370	6.00E−04		[48]
171	79	78	36	96	44	361	1.10E−03		[35]
171	79	78	36	96	44	359	2.00E−03		[35]
171	79	78	36	96	44	363	6.00E−04		[35]
177	81	78	36	102	46	370	3.00E−05		[49]
Proton emitter: p3n channel									
108	53	58	28	54	26	240−−255	5.00E−04		[50]
112	55	58	28	58	28	259	5.00E−04		[51]
146	69	58	28	92	42	287	1.00E−03		[52]
150	71	58	28	96	44	297	2.56E−03		[53]
150	71	58	28	96	44	292	3.05E−03		[54]
160	75	58	28	106	48	300	1.00E−03		[55]
166	77	78	36	92	42	384	6.30E−03		[47]
176	81	78	36	102	46	384	3.00E−06		[35]
Proton emitter: p4n channel									
117	57	58	28	64	30	310	2.00E−04		[56]
117	57	58	28	64	30	295,310	2.40E−04	$+2.40E-04$ $-1.20E-04$	[57]
131	63	40	20	96	44	222	9.00E−05		[58]
141	67	54	26	92	42	285,305	2.50E−04		[58]
141	67	54	26	92	42	315	3.00E−05		[59]
145	69	58	28	92	42	315	5.00E−04		[60]
145	69	92	42	58	28	512	2.00E−04		[61]
155	73	58	28	102	46	315,320	6.00E−05		[62]
165	77	78	36	92	42	384	2.00E−04		[47]
Proton emitter: p5n channel									
130	63	78	36	58	28	432	9.00E−06	$+9.00E-06$ $-4.50E-06$	[63]
140	67	54	26	92	42	315	3.00E−06		[59]
Proton emitter: p6n channel									
121	59	36	18	92	42	240	3.00E−07	$+3.00E-07$ $-1.(0E-07$	[64]
135	65	50	24	92	42	310	3.00E−06		[65]

From this list of possible reactions, it is evident that the experimenter has some choice to use the reaction best suited for the production of the nucleus of interest. However, evidently this choice depends also strongly on the accelerator available, the separation possibilities and much more. For each type of reaction, parameters like the reaction partners and the incident energy have to be optimized in order to achieve the highest production rates of the isotope of interest. For spallation, fragmentation, and deep-inelastic reactions, it is most often advantageous to use a stable nucleus close to the desired final nucleus to enhance the production rate. This choice basically does not exist for fission because only a few quasi stable fissioning nuclei exist. For these reactions, analytical codes have been developed which have a rather good predictive power for the reaction cross sections. Let us mention the EPAX code [1–3] for projectile fragmentation, the SPACS code [4,5] for spallation reactions or the GRAZING model [6,7] for deep-inelastic reactions. The ABRABLA [8,9] code deals with fission, fragmentation, and spallation.

For fusion-evaporation, the situation is different in the sense that all nuclei can be produced with different combinations of projectile, target and incident energy. Therefore, an optimization of these three parameters is needed for any nucleus to be produced. To do so, different codes are available, some of them being analytical, others being of the Monte-Carlo type. In the present work, we have used five codes to calculate fusion-evaporation cross sections: CASCADE [10,11], HIVAP [12], POTFUS + ABLA called CNABLA [13,14,8], PACE [15], and POTFUS + GEMINI++ [14,16]. All codes have advantages and drawbacks and we could not decide a priori which code would perform better over a wide range of nuclei.

The original reason for the present work was to determine production rates for SPIRAL2 where fusion-evaporation reactions were foreseen as a tool to produce neutron-deficient isotopes from mass 20 or so to the heaviest nuclei in the super-heavy element region by means of a target – ion-source ensemble in the production building. The same work was used in the mean time to predict production rates for the S^3 separator [17] or at other facilities. The present work should turn out useful also for fusion-evaporation installations like the Accelerator Laboratory at the University of Jyväskylä [18] or at Tokai in Japan [19].

For this purpose, we performed a literature search of all fusion-evaporation reactions used to produce proton-rich nuclei. Using the projectile-target combination and the energy given in the literature, cross sections were calculated with the five codes. To predict SPIRAL2 production rates, the in-target yields were determined using the predicted primary-beam intensities and the extracted yields were obtained by means of release functions found in the literature. In this way production rates could be predicted for more than 700 proton-rich nuclei.

In order to evaluate the performance of the fusion-evaporation codes and the quality of the production rate predictions, we have performed calculations with all five codes and compared the results to either fusion-evaporation cross sections found in the literature or to production rates. The former values constitute a more direct comparison, however, in most cases the authors had to use transmissions of their separators or release functions which contain quite some uncertainties. For the second type of data, we calculated cross sections and used our own release efficiencies in order to determine in-target production rates and then “released” production rates. The release efficiencies were collected in the frame work of the SPIRAL2 facility [20] where these release functions are needed for fusion as well as fission products.

The purpose of the present paper is to describe the results of this comparison between calculated cross sections or production rates and experimental data for fusion-evaporation reactions. The general outcome is that the different codes overestimate the experimental data by about a factor of 10. Therefore, for e.g. planning an experiment using a fusion-evaporation reaction, the predictions deduced from calculations using fusion-evaporation codes should be reduced by this factor in order to obtain a realistic estimate of the production rates to be expected.

Table 2
Experimental production rates from literature. Given are the mass and charge number of the nuclei of interest and the reference.

A	Z	Ref.	A	Z	Ref.
60	31	[33]	105	49	[68]
61	31	[69]	106	49	[70,71]
62	31	[72]	107	49	[68]
94	47	[73,74]	101	50	[30]
95	47	[75]	102	50	[32]
96	47	[76]	103	50	[77]
97	47	[78]	104	50	[29]
98	47	[79]	105	50	[29]
100	49	[30]	114	56	[34,80]
102	49	[30,81]	116	56	[34]
103	49	[82]	117	56	[34]
104	49	[68]	118	56	[34]

2. Experimental data

In this section, we summarize the experimental data used for the comparison with the theoretical predictions. Table 1 gives the experimental cross sections used in the present work [2].

In general, relatively few fusion-evaporation cross sections are found in the literature and those found have often large error bars or, even worse, no uncertainties at all. This is to a large part due to the fact that the cross sections are often determined at ISOL facilities where information of effusion and diffusion is scarce and induce large uncertainties. Other cross sections are determined by means of mass separators or velocity filters where the transmissions are not well known.

Another problem with a comparison of experimental cross sections and calculated values is that it is often not clear whether the beam energy given is the one at the entrance or in the center of the target. We always use the energy given in the paper for the calculations. If the energy is the one at the target entrance and thus too high compared to the energy in the center of the target, we believe this in not a problem. The maximum of the cross sections is reached at a certain incident energy. At higher energies, the cross sections fall off slowly, whereas at lower energies there is a threshold effect to overcome the Coulomb repulsion which makes that the cross sections fall off much faster on the low-energy side. Therefore, taking in some cases a slightly higher beam energy is somehow on the “safe” side.

Experimental production rates can be found in a number of publications from the former GSI on-line separator [66]. They are summarized in Table 2. Another set of data is available from the work of Korgul et al. [67] in the ^{100}Sn region reproduced in Table 4.

3. Simulation codes

In this section, we give a short overview of the fusion-evaporation codes used to calculate the theoretical cross sections. In total, five codes were used: i) CASCADE, ii) HIVAP, iii) CNABLA, iv) PACE, and v) GEMINI++. These codes use a two-step scenario for the reaction: projectile and target nuclei completely fuse and then decay according to a statistical model approach of compound nucleus reactions. They take into account competition between different decay channels like proton, neutron, and α emission as well as γ decay and fission. All codes give a variety of decay information like the particles emitted, their energy and angular distribution etc. In the present work, we only use the production cross section of the isotope of interest. All programs used the Atomic Mass Evaluation data base from 2012 [83].

[2] The authors are eager to increase the present data base of experimental cross sections and encourage readers to communicate other experimental fusion-evaporation cross sections to us.

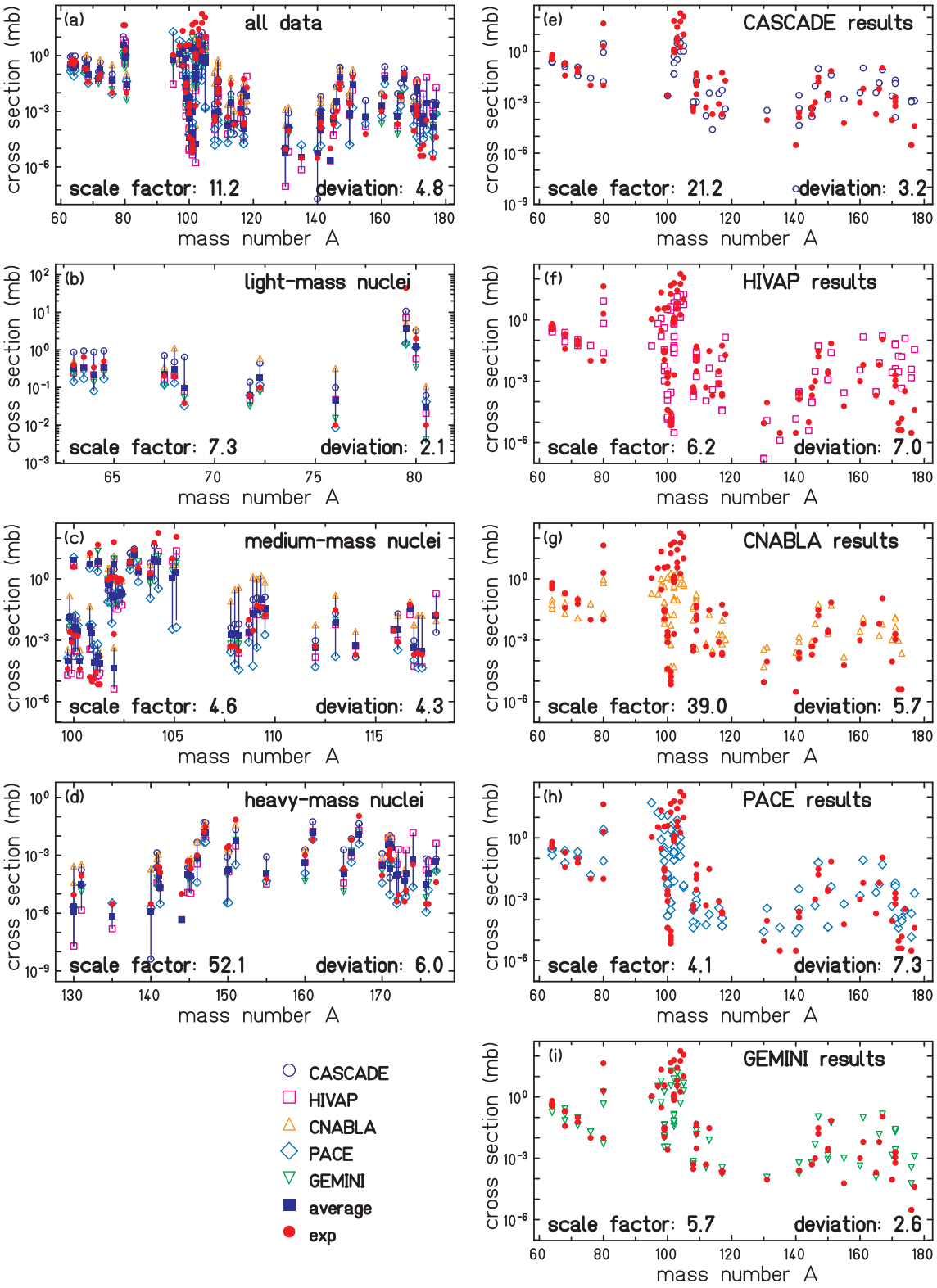

Fig. 1. Comparison of experimental cross sections taken from Table 1 and calculated cross sections with the five different models. Each figure gives the scale factor by which the calculated cross sections had to be divided to match the experimental cross sections. The deviation gives the average difference factor between the experimental cross sections and the scaled calculated cross sections (see text). The left column (a-d) compares the experimental cross sections to all fives model calculations, for all data (a) and for different mass ranges (b–d). The right column compares all experimental data with the different models (e–i).

3.1. The CASCADE code

The program CASCADE was originally written by F. Pühlhofer [10]. The original version of the program was modified by different persons (e.g. E.F. Garman, F. Zwarts and M.N. Harakeh) to perform calculations for special states of good spin and parity, to include isospin and parity properly in the statistical decay as well as to include the electric quadrupole decay.

CASCADE is an analytic program which is quite fast and thus convenient to optimize projectile-target combinations and the beam

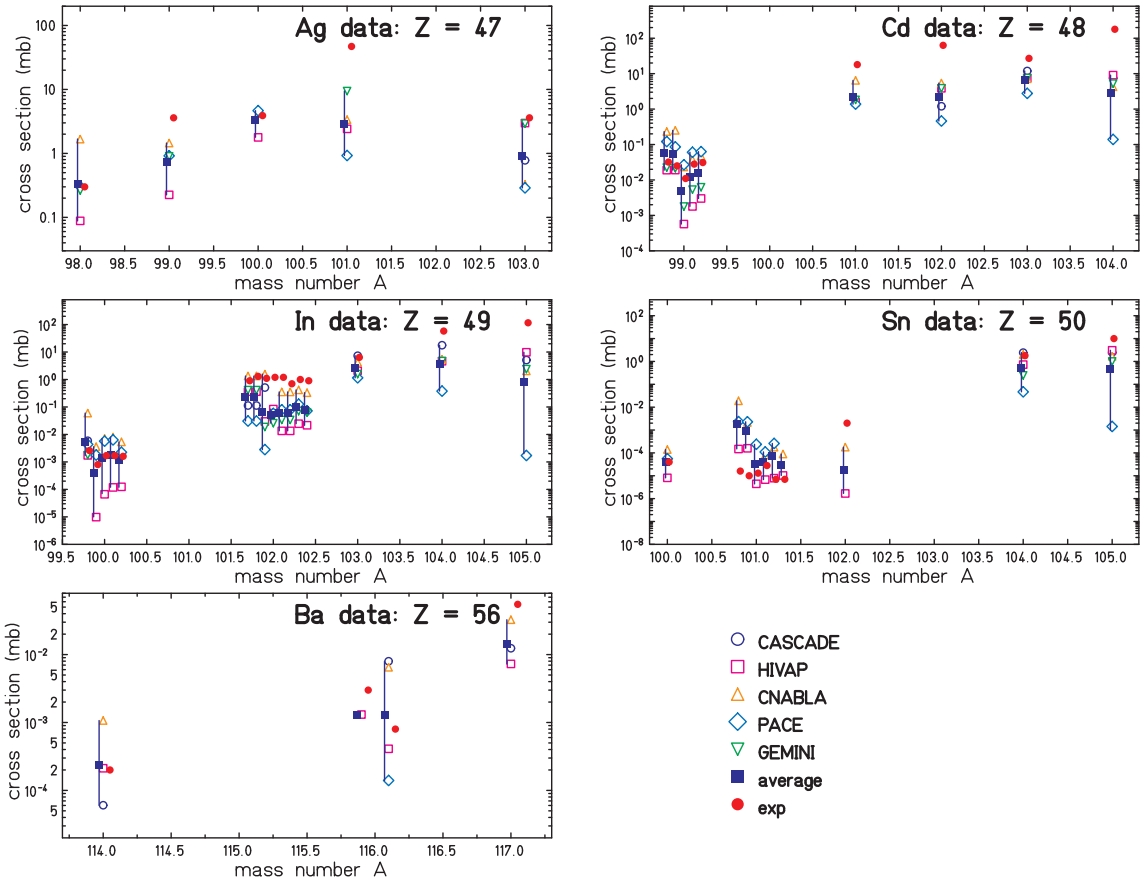

Fig. 2. Comparison of experimental and calculated cross sections (with the adopted scaling factor of 11.2) for selected elements.

Table 3
Scale factors for calculations and deviations between calculated values and experimental data for the five different models in the ^{100}Sn region.

Model	Scale factor	Deviation
CASCADE	6.3	1.9
HIVAP	1.9	3.5
CNABLA	22.8	7.0
PACE	2.1	8.9
GEMINI++	2.4	1.9

energy. In the present work, we use a version of CASCADE provided by D.R. Chakrabarty [11].

3.2. The HIVAP code

HIVAP is a statistical evaporation code written by W. Reisdorf [12]. Several improvements were introduced later [84,85]. We used a version provided to us by F. Hessberger [86]. Like CASCADE, HIVAP is an analytical program being thus very fast.

3.3. The CNABLA code

CNABLA is a program which combines the POTFUS fusion code [14] for the first step of the reaction with the ABLA part from the ABRABLA code [8] for the evaporation. POTFUS is a quite successfully used fusion code and allows us to prepare an input file with a predefined number of events with four parameters: the mass and the charge of the complete-fusion product, its excitation energy and its spin. These events are then used with a special version of ABRABLA [9] to perform the evaporation part by means of a Monte-Carlo technique.

3.4. The PACE code

PACE is probably the most widely used fusion-evaporation code. It was originally written by A. Gavron [15]. This Projection Angular-momentum Coupled Evaporation (PACE) code is again based on the statistical model and uses the Monte-Carlo approach for the de-excitation of the compound nucleus. Only the equilibrium part of the decay is treated, no pre-equilibrium emission is considered.

3.5. The GEMINI++ code

The GEMINI++ code [16] is the C++ version of the original GEMINI code [87,88] written by R.J. Charity. In addition to light particle emission and symmetric fission, it allows for all binary decays to occur. This new version cures problems with heavier systems in the original code. The complete fusion compound nuclei are again produced by the POTFUS code [14] and read into GEMINI++ where a Monte-Carlo procedure is used to perform the de-excitation step.

3.6. Averages from calculations

In order to compare the experimental results to the theoretical predictions from the five codes, some averaging of the calculations is needed. This task is not so easy because the calculations can differ by one or two orders of magnitude from one code to another. A standard average would favor the larger cross sections (e.g. the average of 1 mb and 100 mb being about 50 mb). Therefore, we decided to use the geometrical average yielding for the example above an average of 10 mb. As the uncertainty range we used the maximum and minimum value from all codes.

In general, not all codes give results for all isotopes or all projectile, target, and energy combinations. The average is therefore made with the results available.

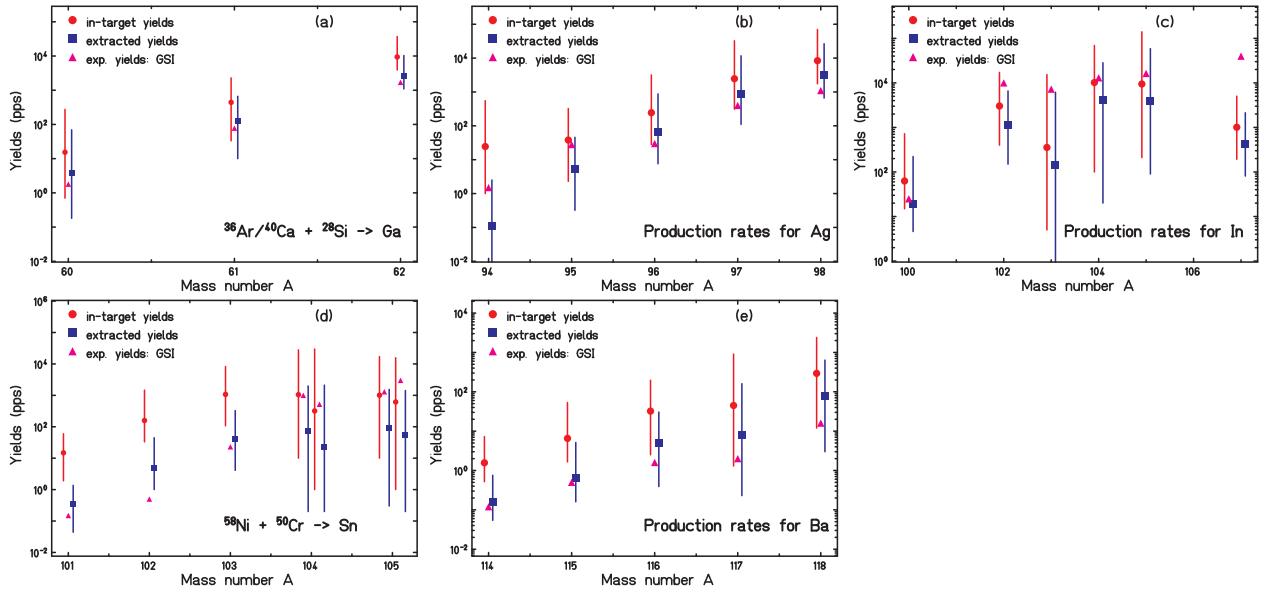

Fig. 3. Comparison of experimental and calculated production rates with a scale factor of 7.3 for the mass A = 60 region (a) and of 4.6 for the mass A = 100 region (b-e). These scaling factors are average values for all models in the respective regions.

4. Results and discussion

4.1. Comparison with experimental cross sections

Fig. 1 gives an overview of all experimental data compared with the results of the individual codes and the averages of these calculations as explained above. As indicated on Fig. 1a to get the best match between the average of the simulations and the experimental data, we had to reduce the results of the calculations by a scale factor of 11.2. The parameter called "deviation" is a measure for the scatter of the calculated cross sections, after scaling, around the experimental ones. Again due to large differences between the calculated values from different models, we used a logarithmic difference defined as:

$$deviation = 10^{**}\left[1/n \sum_{n} abs\left(log_{10}\left(\frac{\sigma_{cal}/sf}{\sigma_{exp}}\right)\right)\right]$$

where n is the number of data points, σ_{cal} and σ_{exp} are the calculated and the experimental cross sections, respectively, and sf is the scale factor mentioned above. Therefore, this deviation is the average factor by which the calculations deviate from the experimental value: the smaller this value is, the better the model calculation, once scaled by a constant factor, agrees with experimental data.

From Fig. 1a, we conclude that the average of the five model calculations corrected by a scale factor of 11.2 deviate on average by a factor of close to 5 for individual value. As can be seen from the left-hand side of the Fig. 1, the scatter between the models and the experimental data is much smaller for lighter nuclei and gets worse when moving to heavier nuclei.

The right-hand side of Fig. 1 gives an analysis of the results as a function of the model used to calculate the cross sections. From a first glance, it seems that PACE is the best model, because the scale factor is the smallest of all. However, the scatter of the data is the largest of all models. Overall we believe that the GEMINI++ model coupled to the POTFUS fusion program gives the most convincing answer for fusion-evaporation cross sections. As in the other cases, the agreement is better for the low-mass region (A < 90) with a scale factor of 3.4 and a deviation parameter of 1.9 and for the medium mass region (90 < A < 130) with values of 2.8 and 1.9.

Interestingly the models which need a large scale factor to match the experimental data, CASCADE and CNABLA, have a reasonably small scatter of the data. This is in particular true for the CASCADE model. HIVAP has a reasonably small scale factor but a very large scatter of the data.

In the ^{100}Sn region, a lot of experiments have been performed and experimental cross sections determined, notably at the former GSI on-line separator [66]. Therefore, this region allows for a detailed comparison of experimental data and calculations. If we use the overall scale factor of 11.2, we obtain a rather good match between experimental data and calculations for the most exotic nuclei (see Fig. 2). However, closer to stability the experimental data are underestimated by the scaled calculations. This statement is valid for all elements from silver (Z = 47) to barium (Z = 56).

An interesting question is certainly, which model predicts best cross sections in the ^{100}Sn region. If we compare the large body of experimental data from A = 94 to A = 117 to the different models, we get scale factors and deviations as given in Table 3. In this region, HIVAP and POTFUS + GEMINI++ give the best results with small scale factors and small deviations. An average scale factor for all models in this region is 4.6.

4.2. Comparison with production rates

Another possibility to compare predictions and experimental rates is to use production rates achieved in experiments and compare them to calculated rates. This comparison is possible with production rates published e.g. from the former GSI on-line separator (see Table 2). However, in such a comparison the uncertainties are expected to be even larger because, in order to calculate these rates, one has to make assumptions about release and ionization efficiencies. This is a rather difficult task, because it involves a lot of chemistry and the on-line rates are known to fluctuate from one run to the other due to often apparently minor differences of the experimental conditions of different experiments.

Nevertheless, we have attempted to predict production rates for the future SPIRAL2 facility at GANIL, be it for neutron-induced fission of ^{238}U or fusion-evaporation reactions for proton-rich nuclei [20]. For this purpose, we have collected experimental parameters of two types: (i) empirical parameterizations of the release fractions based on measured data at different facilities or (ii) parameters from diffusion and effusion laws which then allow the determination of the total release efficiency, as was established by Kirchner et al. studying the

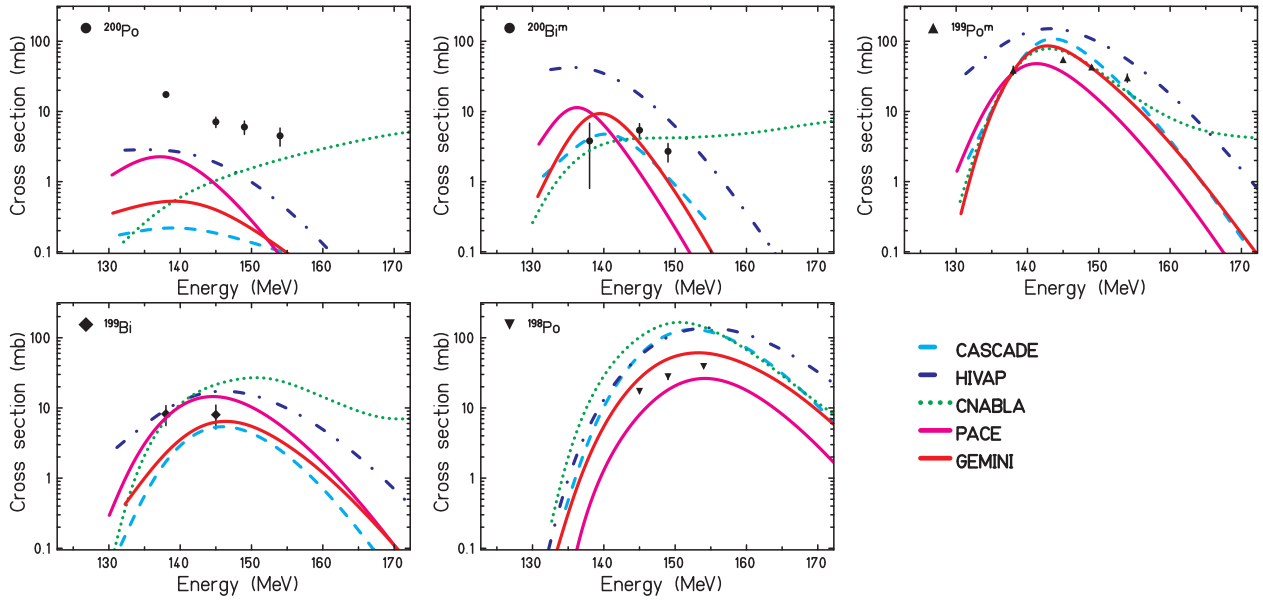

Fig. 4. Comparison of experimental excitation functions for nuclei in the mass A = 200 region [89] with predictions from the five models used. The energy range is unfortunately too small to draw conclusions about the accordance of the maximum of the distributions between experimental data and models.

performances of the UNILAC target ion source systems [90]. The latter approach has been used for the present study, where the diffusion and effusion coefficients were mostly obtained from measurements at UNILAC [90,91], CERN and Dubna [92]. Because of a lack of data in the case of Ga and In, we used diffusion coefficients of the neighboring Ge and Sn elements, respectively. The FEBIAD ionization efficiencies were estimated from efficiencies measured at ISOLDE for rare gases [93]. For the metallic elements of interest, an interpolation in mass gives results which are compatible with the order of magnitude of the efficiencies quoted by Kirchner for UNILAC (30–50% [94]).

Fig. 3 shows the results of this comparison. The in-target yields were estimated from the cross-section averages as described in the previous section. The extracted yields are in-target yields multiplied by the diffusion, effusion and ionization efficiencies, and have to be compared to the experimental production rates measured at UNILAC. As in the case of the production cross sections, the production rates also scatter a lot. However, with the cross section scale factor for the low-mass region of 7.3 (Fig. 3 and 4.6 for the mass A = 100 region (Fig. 3b–e), we reach a reasonable agreement which seems to indicate that a reduction of the calculated cross section is also needed for this comparison.

We note that some of the less exotic isotopes have not been produced in ideal conditions, but experimenters set their apparatus for a short while on these nuclei to start their experiment. As for these nuclei the beam energy was therefore certainly not optimized, the simulation codes may have even larger deficiencies.

4.3. Excitation function of fusion-evaporation cross sections

As mentioned above the body of experimental data for production cross sections is quite scarce. This is even worse in terms of excitation functions where the production cross sections are measured as a function of the energy of the incident beam. We have found one example where sufficient data are available to make a meaningful comparison. In the Bi-Po region [89], a few cross sections have been measured as a function of the incident beam energy, however, only over a short range. In Fig. 4, we compare this excitation function to the different models used in the present work.

Interestingly, if we exclude the CNABLA model for the two A = 200 nuclei, the maximum of the calculated values is rather close for the different models. It is difficult to say whether the experimental trend is reproduced by the model predictions. For such a statement, more data over a wider range of energies would be needed. The figure also evidences that, in case of doubt, a slightly higher energy is more convenient to move away from the threshold effect at low energies.

A large comparison of experimental data in the ^{100}Sn region to HIVAP predictions has been performed by Korgul et al. [67]. These authors measured production rates of nuclei slightly heavier than ^{100}Sn in order to test model predictions in terms of cross sections and of the optimum energy for the production of this nucleus. Therefore, a limited range of incident energies were explored and the rates of different nuclei were determined. The resulting experimental data are given in Table 4. If compared to the method proposed in the present paper for

Table 4
Experimental production rates from Korgul et al. [67]. The reaction ^{58}Ni + ^{54}Fe was used on a 470 μm thick target. The rates are normalised to a beam intensity of 1 pnA.

	^{110}Xe		^{110}I	
Energy (MeV)	rate (1/s)	error (1/s)	rate (1/s)	error (1/s)
190	5.24E−4	1.66E−4	7.50E−3	6.27E−4
200	1.76E−3	3.21E−4	3.52E−2	1.44E−3
205	9.89E−4	1.70E−4	3.30E−2	7.91E−4
210	1.12E−3	2.04E−4	3.89E−2	9.32E−4
215	3.92E−4	6.36E−5	2.00E−2	4.80E−4
220	3.03E−5	3.03E−5	1.11E−2	2.25E−2
	^{109}Te		^{109}I	
Energy (MeV)	rate (1/s)	error (1/s)	rate (1/s)	error (1/s)
205	7.63E−1	2.62E−1	–	–
215	1.43E+1	4.78E+0	7.67E−2	4.69E−3
217	8.93E+0	2.98E+0	8.35E−2	1.04E−3
220	1.26E+1	4.21E+0	4.64E−2	1.25E−3
225	8.71E+0	2.92E+0	5.43E−2	3.51E−3
230	5.37E+0	1.79E+0	2.78E−2	7.59E−4
	^{108}I		^{108}Te	
Energy (MeV)	rate (1/s)	error (1/s)	rate (1/s)	error (1/s)
225	2.95E−4	1.20E−4	0.529	0.016
235	1.46E−3	2.71E−4	0.960	0.007
240	1.70E−3	3.01E−4	1.080	0.008
250	1.09E−3	2.32E−4	0.902	0.007
260	1.73E−3	3.97E−4	0.672	0.008

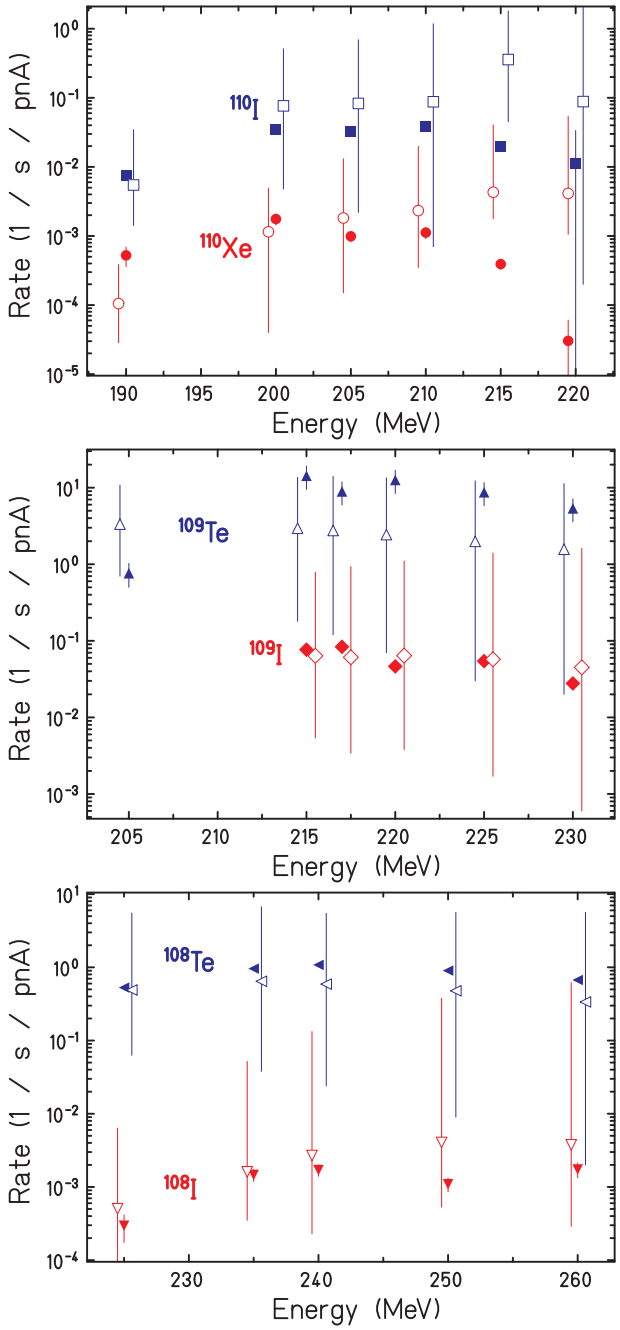

Fig. 5. Comparison of experimental production rates from Korgul et al. [67] with rates calculated with the method described in the present work as a function of the beam energy. Full symbols give experimental data, whereas open symbols correspond to calculated data. The calculated data contain a reduction factor of 4.6.

the calculation of production cross sections for fusion-evaporation reactions, excellent agreement is found for most of the data (Fig. 5). This gives additional confidence in the present method.

5. Summary

We have performed a detailed study of fusion-evaporation cross sections and production rates. Our first finding was that there is a rather limited number of experimental data available in the literature. In addition, these data are most likely subject to large uncertainties keeping in mind that for most of these data no experimental error bars are given in the literature. Therefore, in order to improve the basis for this kind of studies, experimenters need to make efforts to extract cross sections or production rates with experimental uncertainties.

We found that all codes that we tested over-estimate the experimental production cross sections or rates with factors of 4 or more. The most reliable code is maybe the GEMINI++ evaporation code coupled with the POTFUS fusion code, where a relatively small scale factor is needed and a relatively small scatter of the different rates or cross sections is observed once the simulated data are scaled down. The overall overestimation of the cross sections seems to increase towards the heaviest elements. A general recommendation is to divide predicted cross sections or rates by a factor of 5–10 to obtain experimental production rates in reasonable agreement with “experimental reality”, if experimental data are not available.

References

[1] K. Sümmerer, et al., Phys. Rev. C 42 (1990) 2546.
[2] K. Sümmerer, B. Blank, Phys. Rev. C 61 (2000) 034607.
[3] K. Sümmerer, Phys. Rev. C 86 (2012) 014601.
[4] C. Schmitt, K.-H. Schmidt, A. Kelic-Heil, Phys. Rev. C 90 (2014) 064605.
[5] C. Schmitt, K.-H. Schmidt, A. Kelic-Heil, Phys. Rev. C 94 (2016) 039901.
[6] A. Winther, Nucl. Phys. A 594 (1995) 203.
[7] L. Corradi, et al., Phys. Rev. C 66 (2002) 024606.
[8] J.-J. Gaimard, K.-H. Schmidt, Nucl. Phys. A 531 (1991) 709.
[9] A. Kelic-Heil, private communication.
[10] F. Puhlhofer, Nucl. Phys. A 280 (1977) 267.
[11] D. R. Chakrabarty, private communication.
[12] W. Reisdorf, Z. Phys. A 300 (1981) 227.
[13] CNABLA is the POTFUS code coupled to the ABLA evaporation code.
[14] K. Hagino, N. Rowley, A.T. Kruppa, Comp. Phys. Comm. 123 (1999) 143.
[15] A. Gavron, Phys. Rev. C 21 (1980) 230.
[16] R.J. Charity, in Joint ICTP-AIEA Advanced Workshop on Model Codes for Spallation Reactions (IAEA, Vienna, 2008), Report INDC(DNC)-530.
[17] S3 web page at pro.ganil-spiral2.eu/spiral2/instrumentation/s3.
[18] Accelerator Laboratory at the University of Jyväskylä, web page athttps://www.jyu.fi/fysiikka/en.
[19] Tandem Accelerator Section, Department of Research Reactor and Tandem Accelerator, web page athttp://ttandem.jaea.go.jp/index.
[20] GANIL/SPIRAL2 web page at pro.ganil-spiral2.eu.
[21] P. Ennis, et al., Nucl. Phys. A 535 (1991) 392.
[22] S.S.L. Ooi, et al., Phys. Rev. C 34 (1986) 1153.
[23] J. Görres, T. Chapuran, D.P. Balamuth, J.W. Arrison, Phys. Rev. Lett. 58 (1987) 662.
[24] C.J. Lister, et al., Phys. Rev. C 42 (1990) R1191.
[25] S. Skoda, et al., Phys. Rev. C 58 (1998) R5.
[26] S.M. Fischer, et al., Phys. Rev. Lett. 84 (2000) 4064.
[27] B. Varley, et al., Phys. Lett. B 194 (1987) 463.
[28] C.J. Lister, et al., Phys. Rev. Lett. 59 (1987) 1270.
[29] R. Schubart, et al., Z. Phys. A 352 (1995) 373.
[30] M.L. Commara, et al., Nucl. Phys. A 669 (2000) 43.
[31] M. Chartier, et al., Phys. Rev. Lett. 77 (1996) 2400.
[32] M. Lipoglavšek, et al., Z. Phys. A 356 (1996) 239.
[33] C. Mazzocchi, et al., Eur. Phys. J. A 12 (2001) 269.
[34] Z. Janas, et al., Nucl. Phys. A 627 (1997) 119.
[35] H. Kettunen, et al., Phys. Rev. C 69 (2004) 054323.
[36] D. Seweryniak, et al., Phys. Rev. C 60 (1999) 031304.
[37] C.N. Davids, et al., Phys. Rev. Lett. 76 (1996) 592.
[38] G.L. Poli, et al., Phys. Rev. C 63 (2001) 044304.
[39] M. Petri, et al., Phys. Rev. C 76 (2007) 054301.
[40] C.-H. Yu, et al., Phys. Rev. C 59 (1999) R1834.
[41] E.S. Paul, et al., Phys. Rev. C 51 (1995) 78.
[42] S. Hofmann, Part. emission from Nuclei, CRC Press, vol. 2, Chap. 2, 1989.
[43] T. Faestermann, et al., Phys. Lett. B 137 (1984) 23.
[44] D. Seweryniak, et al., Phys. Rev. C 55 (1997) R2137.
[45] C.-H. Yu, et al., Phys. Rev. C 58 (1998) R3042.
[46] R.J. Irvine, et al., Phys. Rev. C 55 (1997) R1621.
[47] C.N. Davids, et al., Phys. Rev. C 55 (1997) 2255.
[48] T. Bäck, et al., Eur. Phys. J. A 16 (2003) 489.
[49] G.L. Poli, et al., Phys. Rev. C 59 (1999) R2979.
[50] R.D. Page, et al., Phys. Rev. C 49 (1994) 3312.
[51] R.D. Page, et al., Phys. Rev. Lett. 72 (1994) 1798.
[52] K. Livingston, et al., Phys. Lett. B 312 (1993) 46.
[53] A.P. Robinson, et al., Phys. Rev. C 68 (2003) 054301.
[54] T.N. Ginter, et al., Phys. Rev. C 61 (1999) 014308.
[55] R.D. Page, et al., Phys. Rev. Lett. 68 (1992) 1287.
[56] F. Soramel, et al., Phys. Rev. C 63 (2001) 031304.
[57] H. Mahmud, et al., Phys. Rev. C 64 (2001) 031303.
[58] C.N. Davids, et al., Phys. Rev. Lett. 80 (1998) 1849.
[59] K. Rykaczewski, et al., Phys. Rev. C 60 (1999) 011301.
[60] J.C. Batchelder, et al., Phys. Rev. C 57 (1998) R1042.
[61] D. Seweryniak, et al., J. Phys. G 31 (2005) S1503.
[62] J. Uusitalo, et al., Phys. Rev. C 59 (1999) R2975.
[63] C.N. Davids, et al., Phys. Rev. C 69 (2004) 011302.

[64] A.P. Robinson, et al., Phys. Rev. Lett. 95 (2005) 032502.
[65] P.J. Woods, et al., Phys. Rev. C 69 (2004) 051302.
[66] R. Kirchner, K.H. Burkard, W. Hüller, O. Klepper, Nucl. Instr. Meth. 186 (1981) 295.
[67] A. Korgul, et al., Phys. Rev. C 77 (2008) 034301.
[68] M. Karny, et al., Nucl. Phys. A 690 (2001) 367.
[69] M. Oinonen, et al., Eur. Phys. J. A 5 (1999) 151.
[70] R. Palit, et al., Nucl. Phys. A 834 (2010) 81c.
[71] A.Y. Deo, et al., Phys. Rev. C 79 (2009) 067304.
[72] B. Blank, et al., Phys. Rev. C 69 (2004) 015502.
[73] C. Plettner, et al., Nucl. Phys. A 733 (2004) 20.
[74] M.L. Commara, et al., Nucl. Phys. A 708 (2002) 167.
[75] S. Harissopulos, et al., Phys. Rev. C 72 (2005) 024303.
[76] I. Mukha, et al., Phys. Rev. C 70 (2004) 044311.
[77] O. Kavatsyuk, et al., Eur. Phys. J. A 25 (2005) 211.
[78] Z. Hu, et al., Phys. Rev. C 60 (1999) 024315.
[79] Z. Hu, et al., Phys. Rev. C 62 (2000) 064315.
[80] C. Mazzocchi, et al., Phys. Lett. B 532 (2002) 29.
[81] M. Gierlik, et al., Nucl. Phys. A 724 (2003) 313.
[82] J. Szerypo, et al., Z. Phys. A 359 (1997) 117.
[83] G. Audi, et al., Chin. Phys. C 36 (2012) 1287.
[84] W. Reisdorf, et al., Nucl. Phys. A 444 (1985) 154.
[85] W. Reisdorf, Z. Phys. A 343 (1992) 47.
[86] F. Hessberger, private communication.
[87] R. Charity, et al., Nucl. Phys. A 476 (1988) 516.
[88] R. Charity, et al., Nucl. Phys. A 511 (1990) 59.
[89] K. Sudarshan, et al., Phys. Rev. C 95 (2017) 024604.
[90] R. Kirchner, Nucl. Instr. Meth. B70 (1992) 186.
[91] R. Kirchner, Nucl. Instr. Meth. B126 (1997) 135.
[92] G. Beyer, E. Hageb, A. Novgorodov, H. Ravn, Nucl. Instr. Meth. B204 (2003) 225.
[93] L. Penescu, R. Catherall, J. Lettry, T. Stora, Phys. Sci. Instr. 81 (2010) 02A906.
[94] R. Kirchner, Rev. Sci. Instr. 67 (1996) 928.